Title

Changing climate and reorganized species interactions modify community responses to climate variability.

Journal

Proceedings of the National Academy of Sciences of the United States of America, 120(39)

Authors

Wang, Junna

Grimm, Nancy

Lawler, Sharon

et al.

Publication Date

2023-09-26

DOI

10.1073/pnas.2218501120

Peer reviewed

PNAS RESEARCH ARTICLE | ECOLOGY
ENVIRONMENTAL SCIENCES

Changing climate and reorganized species interactions modify community responses to climate variability

Junna Wang[a,1], Nancy B. Grimm[b], Sharon P. Lawler[c], and Xiaoli Dong[a]

Edited by Pablo Marquet, Pontificia Universidad Catolica de Chile, Santiago, Chile; received October 28, 2022; accepted August 7, 2023

While an array of ecological mechanisms has been shown to stabilize natural community dynamics, how the effectiveness of these mechanisms—including both their direction (stabilizing vs. destabilizing) and strength—shifts under a changing climate remains unknown. Using a 35-y dataset (1985 to 2019) from a desert stream in central Arizona (USA), we found that as annual mean air temperature rose 1°C and annual mean precipitation reduced by 40% over the last two decades, macroinvertebrate communities experienced dramatic changes, from relatively stable states during the first 15 y of this study to wildly fluctuating states highly sensitive to climate variability in the last 10 y. Asynchronous species responses to climatic variability, the primary mechanism historically undergirding community stability, greatly weakened. The emerging climate regime—specifically, concurrent warming and prolonged multiyear drought—resulted in community-wide synchronous responses and reduced taxa richness. Diversity loss and new establishment of competitors reorganized species interactions. Unlike manipulative experiments that often suggest stabilizing roles of species interactions, we found that reorganized species interactions switched from stabilizing to destabilizing influences, further amplifying community fluctuations. Our study provides evidence of climate change-induced modifications of mechanisms underpinning long-term community stability, resulting in an overall destabilizing effect.

climate change | community stability | compensatory dynamics | community-wide synchronous responses | ecosystem resilience

Significance

Long-term ecological stability plays a critical role in maintaining ecosystem functioning and sustainable delivery of ecosystem services in a varying world. While natural ecological communities can maintain stability through various mechanisms, little is known about how climate change might alter the effectiveness of these mechanisms and their consequences for ecosystem functions and services. Our study shows that the mechanisms historically governing community stability may be largely weakened as climate changes. Some may even flip to a destabilizing force and drive ecological communities to a state of much lower stability and higher sensitivity to environmental fluctuations. These mechanistic insights into community stability shifts can enhance our capacity to better forecast and prepare for upcoming community/ecosystem adjustments under climate change.

Long-term stability of natural ecosystems is critical for the sustainable delivery of ecosystem functions and services. Both theoretical analyses and field observations have shown that natural communities can buffer against environmental fluctuations and maintain temporal stability (as relatively low variance in biomass and species richness) through an array of mechanisms (1–7). Asynchrony in species responses to environmental fluctuations has been widely recognized as a major mechanism underpinning community stability (6, 8–10). This mechanism can produce compensatory dynamics; that is, the decrease in abundance of one species is compensated by increased abundance of other species (11). Biodiversity (number of species) and species interactions such as predation can also reduce temporal fluctuations of community biomass (8, 12, 13). Predation can prevent monopolization or overproliferation of one species, promoting biodiversity and stability (12). In addition, highly resilient dominant species, as a result of their specific life history traits and phenotypic plasticity, also contribute to temporal stability of certain communities (14, 15). Despite this buffering capacity, climate change—including warming and increased frequency and magnitude of extreme events—has modified habitats worldwide, leading to species range and phenology shifts, biodiversity loss, novel community composition, and reorganized species interactions (16–20). Despite these changes being well known, it remains unclear whether the foundational mechanisms underlying community stability are still effective and sufficient to maintain long-term stability.

Under a changing climate, mechanisms historically undergirding community stability could be weakened or become ineffective (21, 22). Within a certain climatic range, a variety of species might thrive under different local climatic conditions, leading to asynchronous species responses to climatic variability. However, if the changing climate deviates far beyond its historical domain, it is likely that most extant native species will be negatively affected, resulting in community-wide synchronous species responses, and eroding asynchrony in species responses and compensatory dynamics. Previous long-term observations show that extreme events can cause extensive mortality of dominant species, introducing nonlinear species responses to the newly altered environment (21). Loss of species or changes in their relative abundances consequently alter species interactions within a community, leading to reorganized species interactions with new network structure and interaction strengths (20). For example, the loss of large, top predators can have cascading effects on lower trophic levels, such as the outbreak of an intermediate trophic level and

Author contributions: J.W., N.B.G., S.P.L., and X.D. designed research; J.W., N.B.G., S.P.L., and X.D. performed research; J.W. analyzed data; and J.W., N.B.G., S.P.L., and X.D. wrote the paper.

The authors declare no competing interest.

This article is a PNAS Direct Submission.

[1]To whom correspondence may be addressed. Email: jnawang@ucdavis.edu.

This article contains supporting information online at https://www.pnas.org/lookup/suppl/doi:10.1073/pnas.2218501120/-/DCSupplemental.

Published September 18, 2023.

the subsequent collapse of the next lower trophic level (23). However, climate change can also introduce novel species into a community, building new links into species interaction networks (19). Great uncertainties remain on whether and under which conditions the reorganization of species interactions will dampen or amplify community responses to increasing climate variability (22). Current understanding about the role of reorganized species interactions has been limited to a few manipulative experiments, whose results often suggest dampening effects (24, 25). For instance, in a grassland experiment, in response to increased precipitation, species richness and biomass increased initially, but later, these positive responses were reversed by reorganized species interactions (24). In stream mesocosms, drought caused partial collapse of a food web, but the reorganized food web preserved its core structure, allowing the community to function as robustly as the previous one (25).

While manipulative experiments are a powerful approach to understand underlying mechanisms, they often suffer from inadequate representations of the complexity of natural ecosystems (21). Communities in natural ecosystems are exposed to multidimensional climate change (e.g., warming, floods, and drought) (26) and are embedded in a larger, more complicated environment where regional climate change alters landscape features such as land cover, exerting regional effects on local communities (21, 27). It is uncertain to what extent results derived from experiments can apply to complex natural communities (22). Direct evidence from long-term observations on the role of reorganized species interactions will provide strong complementary insights, but so far, such evidence is rare. Furthermore, the stability of natural communities is often supported by multiple intertwined mechanisms (28, 29). The weakening of one mechanism may influence the effectiveness of other mechanisms. Interactions such as those between different mechanisms have rarely been explored. In this study, we ask: 1) How does climate change modify the effectiveness of various stabilizing mechanisms—including their direction (stabilizing vs destabilizing) and strength in natural communities? And 2) how do different mechanisms orchestrate novel community dynamics under multidimensional climate change?

To address our research questions, it is essential to have observations or manipulative experiments that cover a sufficiently long period comparable to the timescale of climate change (21, 24, 30). Ecological consequences of climate change are likely to emerge early in ecoregions that are most sensitive to climate change, such as dryland ecosystems (31). Here, we compiled a long-term dataset spanning four decades from Sycamore Creek (*SI Appendix*, Fig. S1), a dryland stream in Arizona (USA) (32). The dataset includes hourly air temperature and daily discharge of 1980 to 2021, along with 18-y monitoring of biotic communities. The biotic data are weekly to monthly measurements of algal, macrophyte, and macroinvertebrate communities in March-July after winter flood disturbances during two periods: 1985 to 1999 (hereafter "historical period") and 2010 to 2019 (hereafter "recent period"). The two periods have 6 gap years (i.e., 1988, 1990, 1991, 1996, 1998, and 2018) due to funding limitation or lack of water in the stream (more information provided in *SI Appendix, Text S1*). In the historical period, mean annual air temperature fluctuated but did not show a significant warming trend (Fig. 1*A*). Interannual hydrology varied widely (Fig. 1*B* and *SI Appendix*, Fig. S2*C*), similar to most streams in arid regions with flashy hydrographs (33, 34). Since 2000, mean annual air temperature at this site increased by 1 °C with a warming rate of 0.05 °C/year (Fig. 1*A* and *SI Appendix*, Fig. S3*A*), comparable to the rate of warming worldwide (17). Along with rising air temperature, this site became drier in the recent period, showing a decreased precipitation by 40% (Fig. 1*D* and *SI Appendix*, Fig. S3*C*) and an increased number of zero-flow days (Fig. 1*E*). Moreover, consecutive 2-y and 3-y droughts became more frequent, especially between 2011 and 2016 (smaller dots and higher bar in Fig. 1*B*, and the wider blue–green area in 2011 to 2016 in Fig. 1*C*; more detailed analysis of hydroclimatic alteration is in *SI Appendix*, Fig. S4 and *Text S2*). These patterns are consistent with increasing drought and climate variability predicted for this region (31, 35). In addition, after the U.S. Forest Service removed cattle grazing from the watershed around 2000, wetland plants began to colonize the stream and their extent has greatly expanded under climate change (36). While the wetland species are not novel to the system (historically abundant before the late 19th century, but later lost by grazing and climate variations) (37), their reestablishment and dramatic increase after 2000 may provide insights into the effect of newly colonizing species, which is expected to become more common with large-scale species range shift under climate change (19). Overall, the distinct hydroclimatic regimes in the historical and recent periods and the recent colonization of wetland species, coupled with comprehensive long-term biological datasets, provide us with the rare opportunity to address our research questions.

In what follows, we first focus on macroinvertebrate community, the consumers of this ecosystem, characterizing temporal stability of community dynamics by comparing the historical and the recent periods. Second, we quantify the level of asynchrony in species–environment interactions and its contribution to compensatory dynamics. Finally, we consider the macroinvertebrate community in a broader context, linking it with primary producers and abiotic environmental factors (i.e., air temperature, winter floods, and summer droughts) through causal network analyses to gain a holistic understanding of how multiple mechanisms interact to enhance or weaken the stability of the entire ecological community.

Results

Dramatically Reduced Interannual Stability of Community Abundance and Biomass. We found that interannual variations in both total abundance and total biomass of the macroinvertebrate community increased dramatically from the historical to the recent period. The coefficient of variation (CV) of total biomass increased by around threefold from 0.35 [90% CI: (0.20, 0.54)] to 1.57 [(0.69, 2.08)] (Fig. 2 *C* and *D* and *SI Appendix*, Fig. S5 *A* and *B*). It is more dramatic in number per wetted stream length, taking into account the expansion and contraction of stream wetted area with hydrology (*SI Appendix*, Fig. S5*C*). The minimum yearly biomass density of the recent period (0.47 g/m^3 in 2013) was only ~45% of that in the historical period (1.04 g/m^3 in 1987). The macroinvertebrate biomass was stuck in this very low level for 3 y between 2013 and 2016 (Fig. 2*D*). In contrast, in the recent period, the maximum biomass density, which occurred in a very wet year 2010 that followed on two wet years (2008 to 2009), was almost six times higher than the maximum of the historical period, that is, 47.53 g/m^3 (2010) vs. 7.41 g/m^3 (1992). Such increased community fluctuations were also observed at another two sites several kilometers upstream and downstream of our focal study site (*SI Appendix*, Figs. S6 *C* and *D* and S7), indicating that this was likely a pattern across the whole system. In addition to the increased community fluctuations, results from Bayesian multiple regressions suggest that in the recent period, total biomass of the macroinvertebrate community became very sensitive to the intensity of summer drought (Fig. 2*B*) and mean annual air temperature (*SI Appendix*, Fig. S8). The increased magnitudes of fluctuations and sensitivity to climatic variability in the recent

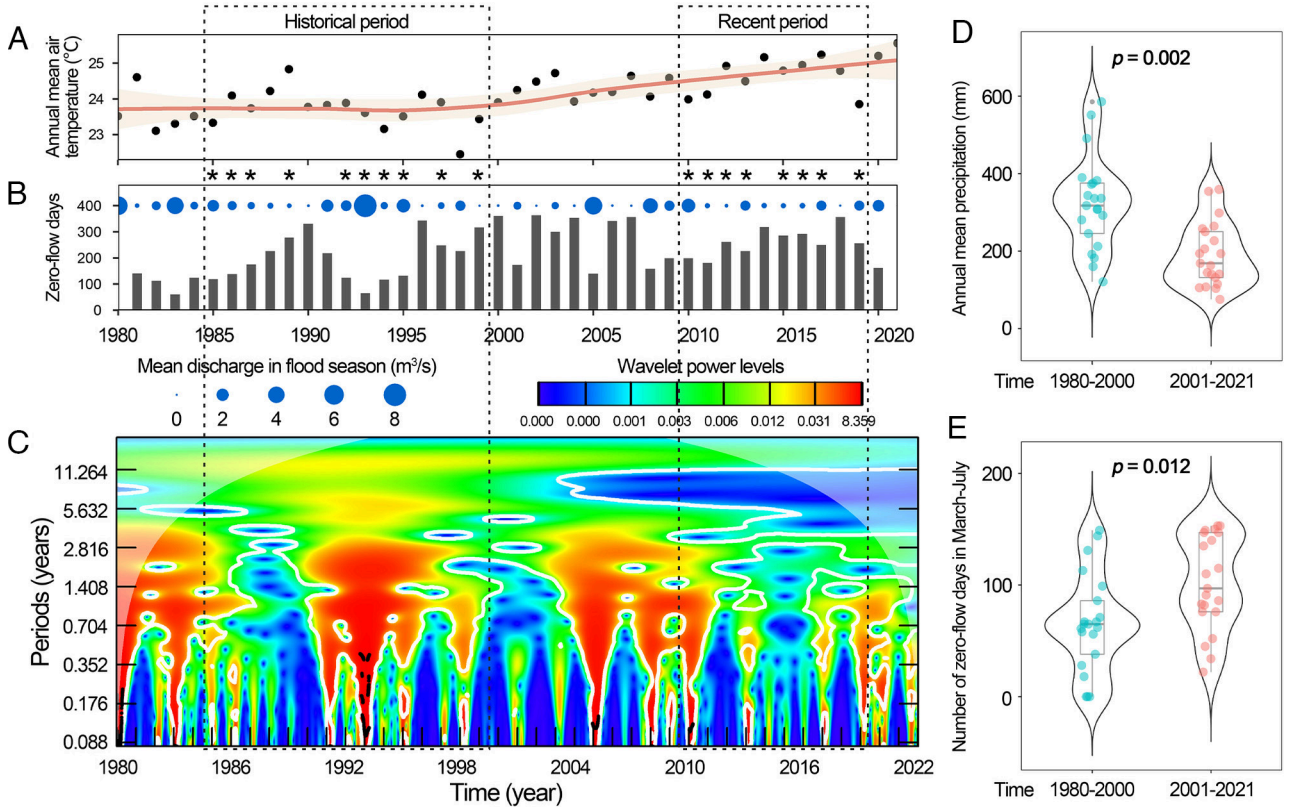

Fig. 1. Characteristics of the four-decade climatic and hydrologic regimes in Sycamore Creek (AZ): (*A*) mean annual air temperature, (*B*) number of annual zero-flow days in the stream to represent drought intensity (bars), and mean discharge during the winter flood season (October-March) to represent flood magnitude (area of blue points), (*C*) wavelet power variations of mean daily discharge over time, (*D*) comparison of annual mean precipitation between the two periods, and (*E*) comparison of number of zero-flow days in sampling season (March-July) between the two periods. Wavelet power spectrum is generally proportional to the magnitude of flood events, that is, dry years are characterized by lower spectrum denoted in blue–green colors in (*C*). Note that after around 2011, the red signal (i.e., high wavelet spectrum indicating floods) between the periods of 1 to 3 y almost disappeared, indicating the emergence of consecutive 2 to 3-y droughts. Stars below (*A*) indicate the years with macroinvertebrate observations. The *P* values in (*D* and *E*) indicate the significance level of change between the two periods by the *t* test with equivalent sample sizes.

period contrast with the patterns in the historical period, when total biomass of macroinvertebrates was not correlated with either drought intensity or air temperature (Fig. 2*A* and *SI Appendix*, Fig. S8) and hence was relatively stable from year to year (Fig. 2*C*), regardless of the high interannual variability in hydrology (Fig. 1*B*).

Asynchronous Species Responses to Climate Variability Undergirding Historical Community Stability. To gain better insights into the underlying mechanism of such a shift in community response to the environment, we used Bayesian multiple regressions with antecedent effects (38) to quantify the total effect of hydrological conditions on the eight taxonomic groups of macroinvertebrates (Fig. 2 *A* and *B*). We found that asynchronous species responses to climatic variability played a critical role in stabilizing the macroinvertebrate community in the historical period. Odonata (large top predators) and Ephemeroptera (collector-gatherers) flourished in wet years, with their abundance significantly, negatively correlated with the severity of summer drought (measured as the number of zero-flow days in the sampling season; points in Fig. 2*A*). Coleoptera (collectors and predators) and Gastropoda (grazers and collectors), on the contrary, were abundant in dry years with their abundance significantly, positively correlated with the severity of summer drought. The abundances of these four groups were largely associated with summer hydrology of the current year (bars in Fig. 2*A*), with negligible effects of antecedent conditions. While Oligochaeta (worms) also preferred dry years, they were more responsive to summer hydrology of the preceding year (bars in Fig. 2*A*). The abundances of the remaining three groups, Trichoptera, Lepidoptera, and Diptera, were not correlated with hydrological conditions. Such diverse responses to summer drought not only occurred at the class/order level but also existed at a finer taxonomic resolution, i.e., diverse responses by different families/genera within an order (e.g., within Ephemeroptera, Diptera, and Coleoptera) (*SI Appendix*, Table S1). As a result of the mixed correlations (negative and positive) between the hydrological condition and abundances of different macroinvertebrate groups, the total biomass each year was not significantly correlated with hydrological conditions and was relatively stable (Fig. 2 *A* and *C*). Such asynchronous species responses likely generated compensatory dynamics. The variance ratio (VR), a metric to quantify compensatory dynamics (11), was equal to 0.88 (<1 denotes the presence of compensatory dynamics) and ~60% of taxa–taxa covariances were negative (*SI Appendix*, Fig. S9*A*). By resampling the observed community composition data in the historical period with the block bootstrapping method, the probability of VR < 1 was ~70 %. These results suggest a high likelihood of compensatory dynamics occurring in the historical macroinvertebrate communities.

Shifting from Asynchronous to Synchronous Responses to Climate Variability and Reduced Species Richness in the Recent Period. In the recent period, these mixed correlations between drought and macroinvertebrate abundance were replaced by solely negative correlations for almost every group (Fig. 2*B* and *SI Appendix*, Table S1). Severity of summer drought still had a significantly negative effect on Odonata and Ephemeroptera, but the effect sizes were ~3 to 15 times greater. Diptera, a large group of usually

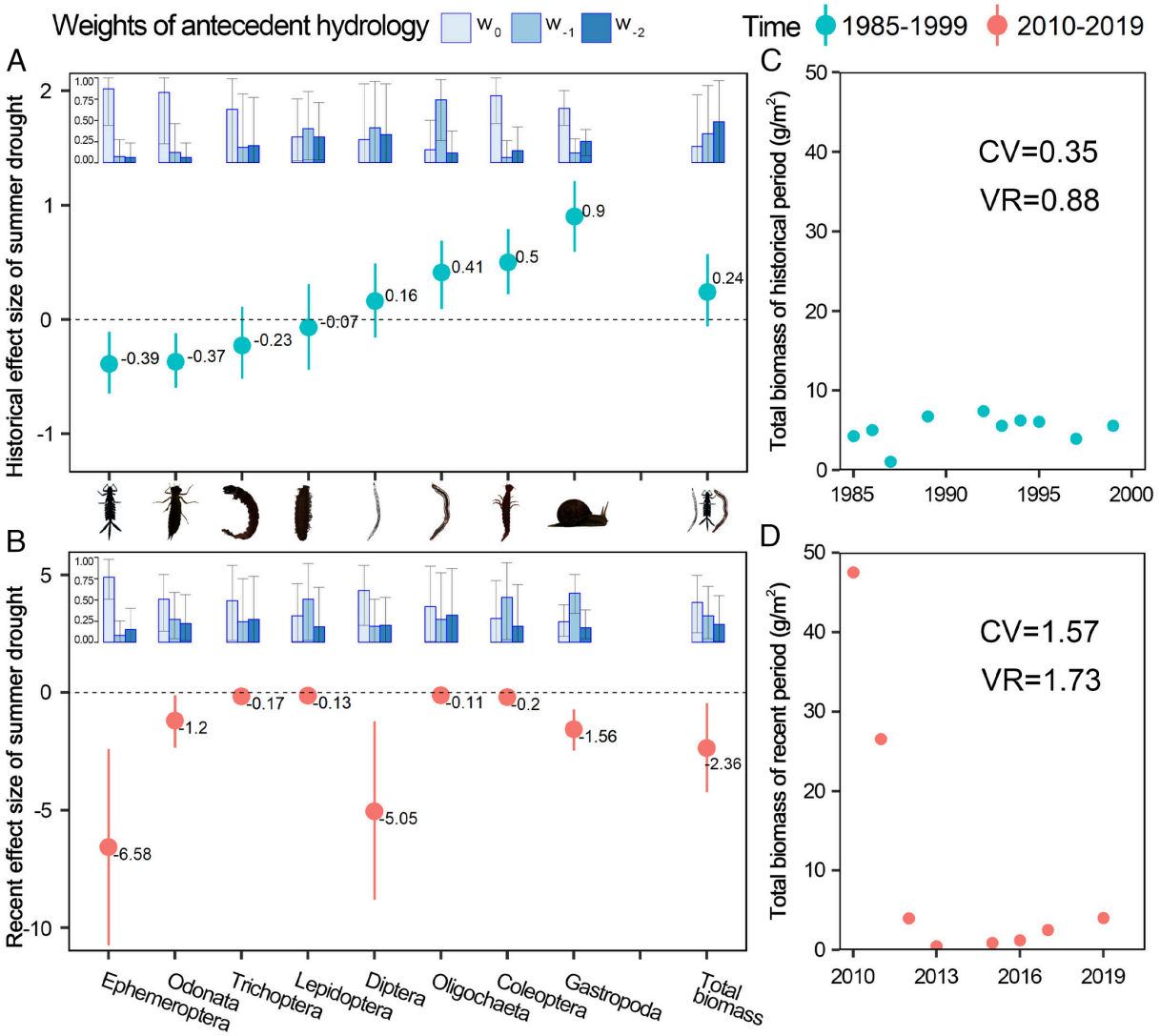

Fig. 2. Total and antecedent effects with mean and its ±90% credible intervals of summer drought (measured as the number of zero-flow days during the post-winter flood sampling season) on macroinvertebrate abundance in the (*A*) historical period (1985 to 1999, $n = 90$) and (*B*) recent period (2010 to 2019, $n = 28$), and yearly macroinvertebrate community dynamics (total biomass) in the (*C*) historical and (*D*) recent periods. Here, w_0 is the weight (relative importance) of current year's hydrology; w_{-1} is the weight of last year's hydrology; and w_{-2} is the weight of second last year's hydrology. CV is coefficient of variation, higher CV indicating lower temporal stability. VR is variance ratio: VR < 1 represents compensatory dynamics, and >1 denotes synchronous dynamics. Credible intervals were inferred by Bayesian methods.

small-sized macroinvertebrates, became highly sensitive to the intensity of summer drought (Fig. 2*B*), with the abundance in the wet year 2010 12 times higher than the average value over the historical period (*SI Appendix*, Fig. S10). Gastropoda, whose abundance was higher in drier years according to historical observations (Fig. 2*A*), instead showed a significantly negative correlation with the severity of summer drought in the recent period (Fig. 2*B*). Moreover, Gastropoda were more correlated to the drought intensity of both current and antecedent years, suggesting potentially cumulative negative effects of multiyear droughts. The correlation between summer drought and the abundance of Coleoptera, a fraction of which (e.g., adult Dytiscidae) were likely predators of Gastropoda (39, 40), also switched from positive to negative. Such sweeping negative responses to the severity of summer drought led to the dominance of positive taxa-taxa covariances (*SI Appendix*, Fig. S9*B*) and synchronous dynamics in the community (VR = 1.73 with a 90 % CI of [1.22, 2.96] and VR > 1 denotes synchronous dynamics). Together, they dramatically amplified interannual variability in community abundance and biomass.

The synchronous negative responses to summer drought were accompanied by reduced taxa richness and simplified community structure (Fig. 3). We found that taxa richness in the recent period was significantly lower than that of the historical period ($t = 2.758$, $df = 9.684$, $P = 0.021$), especially in these consecutive dry years (2012, 2015 to 2016; Fig. 3 *A* and *B*). Ordination analysis shows that macroinvertebrate community composition in normal and wet years was similar across historical and recent periods (uncircled points toward the *Bottom Left* in Fig. 3*C*). However, community structure in recent dry years was distinct from the historical dry years (left ovals in Fig. 3*C*) and was greatly simplified, dominated by small-sized Diptera and Oligochaeta (right oval in Fig. 3*C*). In dry years (e.g., 1989 and 1999) of the historical period, although the abundance of species that prefer wet years such as Ephemeroptera and Odonata decreased, they were present almost every year (*SI Appendix*, Fig. S11 *A* and *B*). However, these species were extirpated in consecutive dry years of the recent period (see the red box in *SI Appendix*, Fig. S11 *A* and *B*). The synchronous dynamics and the reduced taxa richness emerging in the recent period imply that

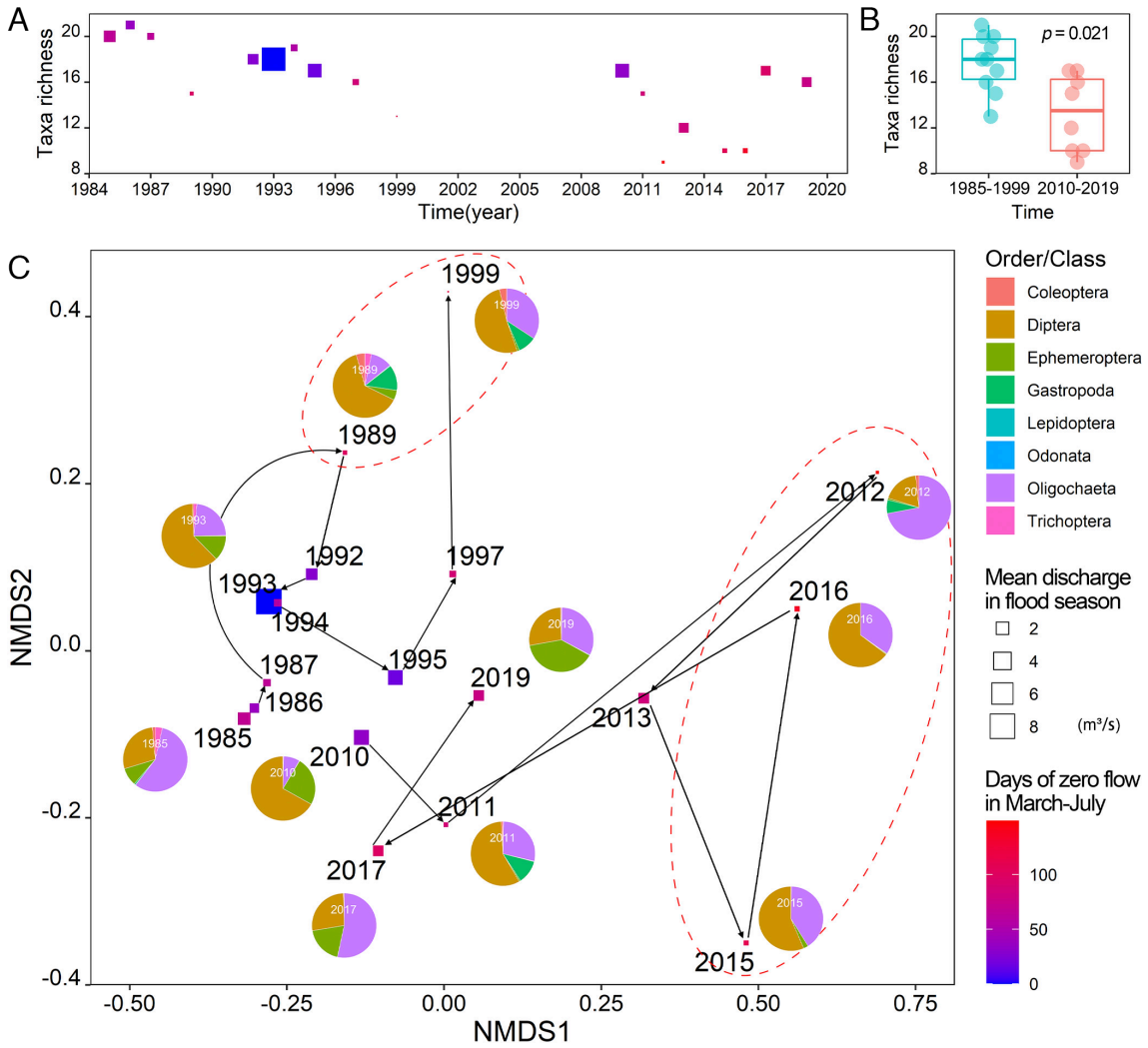

Fig. 3. Year-to-year variation in taxa richness (*A*); significant decline in taxa richness across the historical and recent periods (*B*); and year-to-year structural dynamics of macroinvertebrate communities over the historical (1985 to 1999) and recent (2010 to 2009) periods revealed by nonmetric multidimensional scaling (NMDS) (*C*). In (*A* and *C*), size of squares represents the magnitude of winter flood, and the color of squares denotes the severity of summer drought. The *P* value in (*B*) denotes significance level of richness change between the two periods by the *t* test with equivalent sample sizes. In (*C*), the distance between squares represents the dissimilarity of community structure between years; pie charts show the community composition for select years (community composition for each year is in *SI Appendix*, Fig. S12); and dashed ovals delineate two distinct community structures in dry years.

the system might have undergone profound changes in its abiotic environment or species interactions or both.

Synergetic Effects of Multidimensional Climatic Change Driving the Shift in Species Responses to Climatic Variability. The synchronized species responses to climate variability and reduced taxa richness likely resulted from synergetic effects of multidimensional climatic change—co-occurrence of warming and drought. Structural causal modeling (Fig. 4) shows that the two major external drivers of our study system, air temperature and hydrological conditions (winter flood and summer drought), became increasingly correlated since 2000, when air temperature started to show a clear warming trend (*SI Appendix*, Fig. S13 and Fig. 1*A*), leading to a synergistic effect. This contrasts with the historical period when the two drivers were largely independent (Fig. 4 *A*, ① and ②). When dry years cooccurred with hot years, the severity of summer drought was greatly intensified by multiple pathways (Fig. 4 *B*, ①–⑥). Warming directly elevated stream evapotranspiration. On top of that, decreased precipitation and lower flood magnitude (*SI Appendix*, Fig. S4) facilitated the expansion of macrophytes and wetland plants (hereafter referred to as "macrophytes" collectively; see *SI Appendix*, Table S2 for dominant plant species) in the stream (Fig. 4 *B*, ④). Collectively, they induced much higher evapotranspiration and a much intensified summer drought in dry and hot years (36). The synchrony of warming and drought, particularly in consecutive dry years (e.g., 2014 to 2016), might have formed a new climate that could dramatically alter stream habitats, exerting strong negative effects on most species. For example, in a very dry year (2018), we found that water temperature increased linearly with air temperature, reaching a daily mean temperature >30 °C in June and July (*SI Appendix*, Fig. S14*A*). However, in wet years (2019 to 2020), water temperature increased linearly with air temperature to a certain degree and then leveled off, resulting in daily mean water temperature <23 °C throughout the year (*SI Appendix*, Fig. S14 *B* and *C*).

Reorganized Species Interactions Further Destabilizing Communities. Reorganized species interactions, including altered competition dynamics among primary producers (algae and macrophytes) and its propagating effect onto producer-consumer relationships, became a destabilizing force in the recent period. Historically, algae were the predominant primary producers

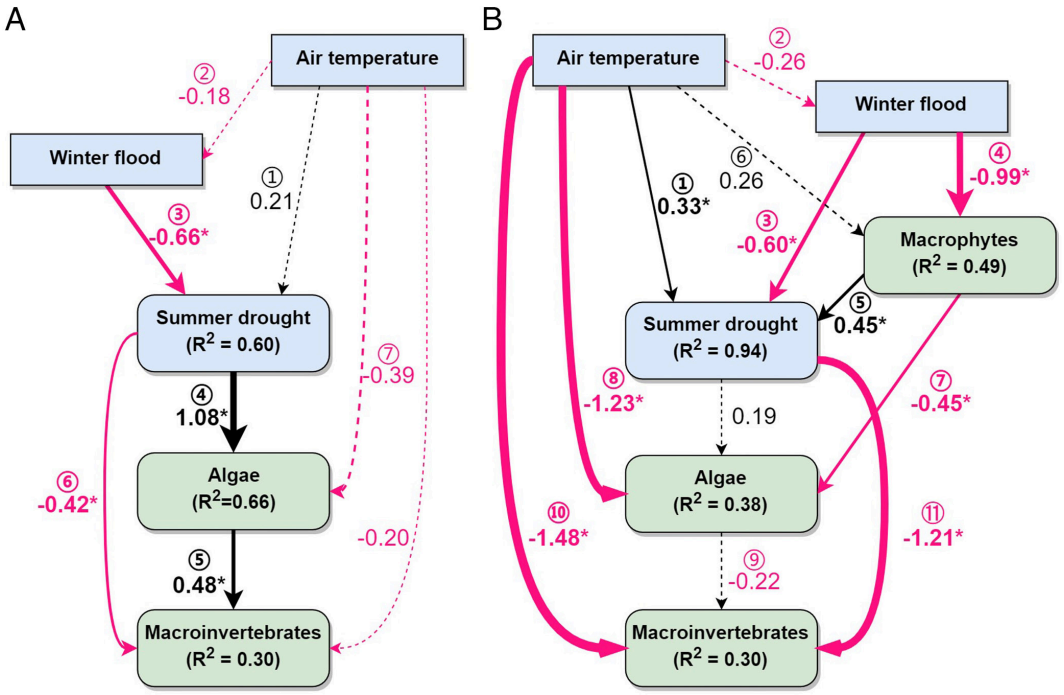

Fig. 4. Causal networks among abiotic and biotic components of the Sycamore Creek ecosystem in the (*A*) historical period (1980 to 2000, *n* = 21 for yearly abiotic data, *n* = 86 for algae, *n* = 90 for macroinvertebrates), and (*B*) recent period (2001 to 2021, *n* = 21 for yearly abiotic data, *n* = 37 for algae and macrophytes; *n* = 28 for macroinvertebrates). Arrows represent a direct causal link. The number adjacent to each line denotes the effect size of that causal link. If an effect size is statistically significant at the 90% credible interval, the effect size is labeled with a star, and the arrow is a solid line; otherwise, the arrow is a dashed line. Black lines represent positive correlations, and red lines represent negative correlations. Line width is proportional to the effect size. "Air temperature" is represented by mean annual air temperature. "Winter flood" is calculated with mean discharge in the winter flood season (October-March). "Summer drought" is quantified by the number of zero-flow days in the sampling season (March-July). Macrophytes refers to mean coverage width of macrophytes and wetland plants along transects. As macrophytes colonized the system after cattle removal in 2000, we only included it in the causal network (*B*). "Algae" is represented by mean chlorophyll a concentration, and "Macroinvertebrates" refers to total biomass of macroinvertebrate communities.

(coverage > 90%, *SI Appendix*, Fig. S15) and the main food sources of macroinvertebrates in Sycamore Creek (33). Algae were highly resilient to winter floods—they recovered rapidly from floods and were prevalent in the entire wetted stream area over the after-winter flood succession (May to July) (*SI Appendix*, Fig. S16*A*) (4, 33). The high resilience and abundance of the algal community underpinned stability of the macroinvertebrate communities in the historical period, with macroinvertebrate biomass significantly correlated with algal abundance (Fig. 4 *A*, ⑤). The resilient primary producers provided a stable foundation for the functioning of asynchronous species responses to climate variability and compensatory dynamics in the consumer (macroinvertebrate) community.

In the recent period, however, the expansion of macrophytes imposed strong, negative effects on algal growth (Fig. 4 *B*, ⑦), and the stability of the algal community at both interannual and seasonal scales decreased (*SI Appendix*, Figs. S15 and S16*B*). Apart from 2010 (a wet year with few macrophytes in the stream), which resembled algal patterns in historical years, in normal and dry years, although algae still peaked in May, algal coverage declined to nearly 0% in July (*SI Appendix*, Fig. S16*B*), presumably outcompeted by macrophytes owing to shading and nutrient competition. With algae declining in abundance and increasing in sensitivity to climatic variability (Fig. 4 *B*, ⑨), macroinvertebrate biomass was no longer directly correlated with algal abundance (Fig. 4 *B*, ⑧). As a result, the effect of macrophytes on macroinvertebrates via algae was relatively small (Fig. 4 *B*, ⑦ and ⑧), compared to the strong direct effects of the environment (air temperature and summer drought; Fig. 4 *B*, ⑩ and ⑪). Since algae are more nutritious than macrophytes for higher trophic levels (41), the loss of the association with such a historically stable, high-quality food source further undermined the stability of the macroinvertebrate communities.

Discussion

Modification of Mechanisms Governing Community Stability. We found that as annual mean air temperature increased by 1°C and precipitation reduced by 40% over the past two decades, warming combined with prolonged, multiyear drought drove macroinvertebrate communities in a dryland stream to a new state of much lower stability and much higher sensitivity to environmental fluctuations. We show that historically, algae as stable primary producers providing a stable food source for consumers (macroinvertebrates), combined with asynchronous responses of consumers to climate variability (Fig. 5 *C* and *E*), gave rise to community stability as low variation in biomass and richness. The asynchronous responses occurred both at the family/genus level within the same order (*SI Appendix*, Table S1) and across different orders/classes (Fig. 2 *A* and *B*). These mechanisms have also been commonly evoked to explain community stability in other ecosystems empirically (8, 12, 28, 42) and theoretically (6, 7, 9, 10). Furthermore, these mechanisms do not act independently. The stability of primary producers and their tight coupling with consumers support asynchronous responses of consumers to climate variability. Because of the stable and abundant supply of primary producers, the decreases of some groups of macroinvertebrates in a fluctuating environment could be compensated by the increases of other consumer groups, maintaining the overall community stability (Fig. 5 *E* and *G*).

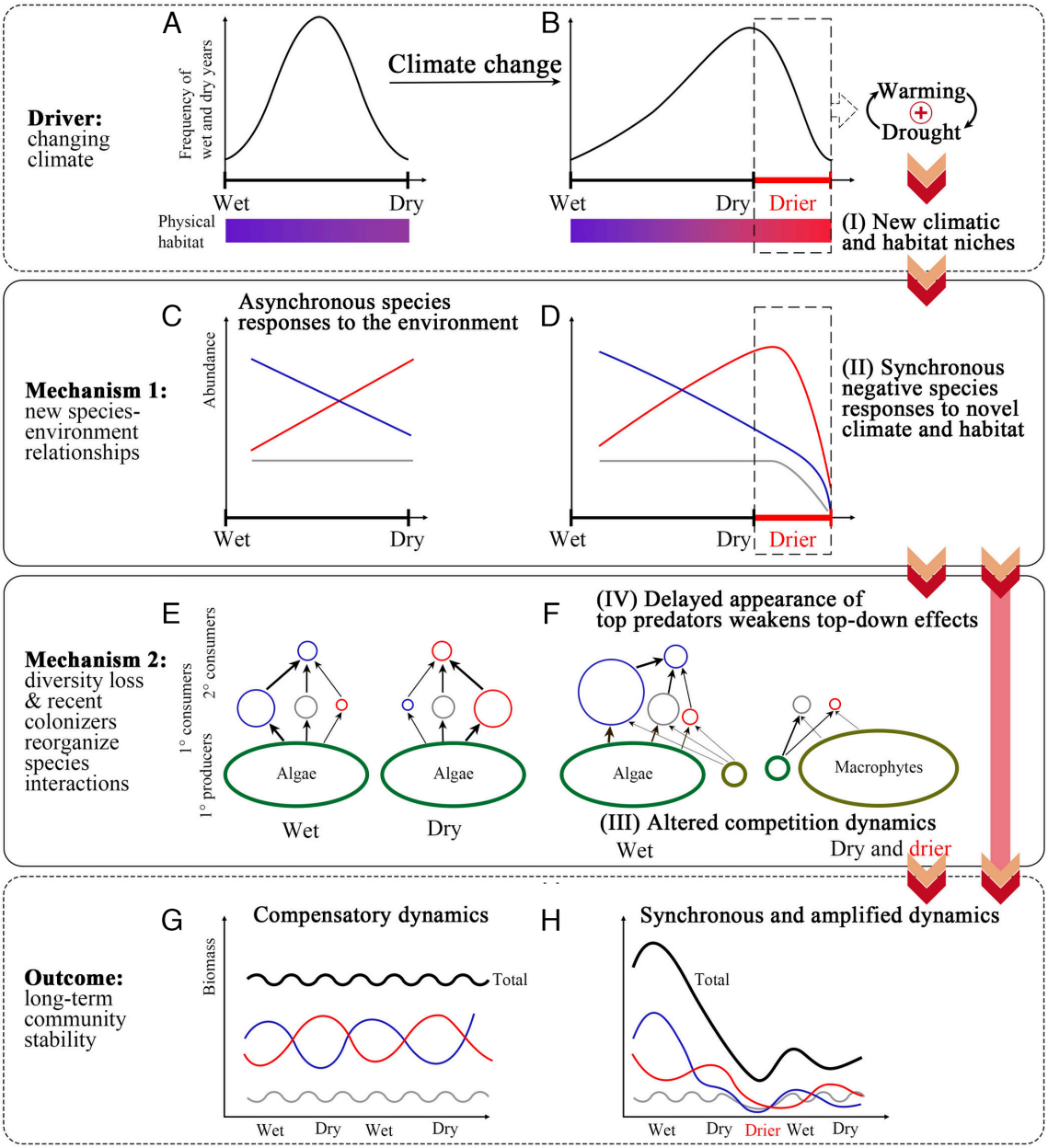

Fig. 5. Conceptual diagram of how various mechanisms buffer or amplify community sensitivity to climate variability. (*A* and *B*) Climate change alters the magnitude and frequency of climatic variability, creating new climatic and habitat niches in dry years by warming-drought feedbacks; (*C* and *D*) Shift from asynchronous species environmental responses to synchronous species responses; (*E* and *F*) Reorganization of species interactions and its amplifying effects by altered competition and delayed predators; and (*G* and *H*) transition from compensatory dynamics to synchronous dynamics as a result of new species-environment relationships and species interactions. In (*C*–*H*), blue lines and circles indicate taxa preferring wet years, red ones indicate taxa preferring dry years, and gray ones indicate taxa historically insensitive to the environment. Color arrows indicate the cascading effects of climate change.

Within a new climate domain, however, these mechanisms became less effective or failed completely. We found cascading effects of climate change on the effectiveness of these stability mechanisms (color arrows in Fig. 5). The cascading effects were initiated by the synergetic effects of warming and drought, particularly the multiyear drought, which can dramatically alter habitats (Fig. 5*B*). The extent of alteration likely exceeded tolerances of most species, triggering community-wide, nonlinear species responses to the environment beyond a threshold (Fig. 5*D*). Such synchronized negative responses reduced species richness (Fig. 5*F*) and total biomass (Fig. 5*H*) in dry years. The reduction of species richness combined with the newly established wetland species led to reorganization of species interactions (Fig. 5*F*). However, under the new climate regime, reorganized species interactions did not dampen but further amplified synchronized species responses to environment fluctuations. Given these cascading effects, long-term community dynamics shifted from compensatory dynamics to synchronous dynamics. Below, we discuss two key components of the cascading effects.

The cascading effects are triggered by climate change altering habitats to the degree that most species might not thrive or survive in them, resulting in synchronized nonlinear species responses. Such dramatic habitat change can be created by pulse-type extreme events (21), synergetic effects of multistressors, and simultaneous effects of climate change from local and regional scales (43). As shown in our study, although the mean annual air temperature differences between a hot and a normal year are <2 °C (Fig. 1*A*), water temperature differences can be amplified by up to 10 °C during the

summer drought season if a hot year co-occurs with drought (*SI Appendix*, Fig. S14). Drier years facilitate the growth of much more extensive macrophytes which slow down flows and increase evapotranspiration (36, 37); thus, the rate of surface water loss by already high evaporation in hot years is exacerbated by rapid transpiration. This results in lower stream discharge and spatially intermittent flow of small, scattered patches, which can dramatically increase stream temperature and reduce dissolved oxygen concentration (40, 44–46). Furthermore, at the watershed scale, the concurrence of warming and drought facilitated the expansion of shrubs/scrubs in replacement of evergreen forests (*SI Appendix*, Fig. S7 and Table S3), likely reducing watershed water storage, groundwater level, and cold water refuge for species (35, 47). In response to habitat change, all taxa were negatively affected by droughts (Fig. 2*B*). While some taxa (e.g., Gastropoda and Coleoptera) increased their abundance in dry years when the degree of drought was within a certain range (Fig. 2*A* and *SI Appendix*, Fig. S11*C* in 1989, 1999, 2011, and 2012), we found that above a threshold, their abundance started to decline remarkedly (*SI Appendix*, Fig. S11*C* in 2013 to 2016). This indiscriminate negative effect of drought substantially decreased taxa richness and promoted the establishment of macrophytes (Fig. 3).

With overall reduction in macroinvertebrate richness and the establishment of macrophytes, reorganization of species interactions further reduced community stability. We show that, in recent dry years, macrophytes outcompeted the historically stable algal community. The outcome of this competition dynamics might have induced the lowered abundance and richness of macroinvertebrate community in dry years (the right food web in Fig. 5*F*). More importantly, the decrease in macroinvertebrate taxa richness, induced by consecutive dry years, might have contributed to the dramatic increase in total biomass of macroinvertebrate community in wet years after dry periods. We observed that total biomass in recent dry years is much lower than that in similar dry years in the historical period, but the wet-year total biomass in the recent period is much higher than similar wet years in the historical period (Fig. 2 *C* and *D*). We speculate that such amplified biomass fluctuations are associated with reorganized species interactions. In consecutive dry years, species that prefer wet years disappeared (*SI Appendix*, Fig. S11 *A* and *B*). This contrasts with the historical period—while their abundance decreased in dry years, they persisted almost every year. Their persistence in dry years, although at low abundance, provides "storage" effects in the system (48), allowing these species to bounce up rapidly in wet years. However, such storage effects were weakened or even undermined under climate change, in which case, it might take longer for the removed species to return when conditions improve (e.g., a wet year). If these species played an important role in community stability, the loss of the storage effects can be consequential (1, 49). For instance, we found that in the recent period, Odonata were first observed with a delay of ~1 mo compared to the historical period (*SI Appendix*, Fig. S17). As large top predators, Odonata (>95% are Anisoptera) feed on many other macroinvertebrates (fish abundance is low, especially in the recent period and most are small minnows), including the often-abundant Diptera, Ephemeroptera, and Oligochaeta (50, 51). Their delayed appearance might cause cascading trophic effects in wet years (23, 40, 50)—the surge in the abundance of their prey, Diptera and Ephemeroptera, the two groups that are most sensitive to air temperature and hydrology (*SI Appendix*, Table S4 and Figs. S8 and S10 and Fig. 2 *B* and, and the left food web in Fig. 5*F*). This is analogous to phytoplankton-zooplankton uncoupling as a result of delayed zooplankton observed in lakes with climate warming (30). Therefore, if changing climate significantly reduces species richness and abundance of functionally important species, the shrinkage of species storage effects might create a legacy effect on community composition in the following years, amplifying community fluctuation over a longer period.

Comparing Long-Term Observations with Manipulative Experiments. Our long-term observations reveal cascading effects of climate change that significantly reduced community stability, mediated by decreased species richness and recently colonizing species. We show that reorganized species interactions further destabilized the community. This contrasts with findings from manipulative experiments that often show stabilizing effects of species interactions (24, 25). Manipulative experiments and long-term observations are two powerful and complementary approaches to investigating how ecosystems work (21). Manipulative experiments excel at teasing apart confounding effects and examining causal effects of single or a few factors, while long-term observations provide the advantage of examining comprehensive and realistic effects. However, with regard to our research question—how climate change alters the effectiveness of stability mechanisms—so far, our understanding has been disproportionally derived from manipulative experiments. These experiments mostly manipulated one stressor and focused on local effects; therefore, they might not well represent synergetic effects of multidimensional climate change, the combined local and regional effects, or the colonization of newly arrived species. Our long-term study found that these factors working together could trigger the cascading effects of climate change on natural communities, which have rarely been captured in manipulative experiments.

A common pitfall of long-term observations of natural communities is confounding factors. Particularly relevant to our study is the removal of cattle from the watershed in 2000 (see *SI Appendix, Text S3* for detailed discussion on other potential confounding factors). The most significant response was the encroachment of macrophytes along the stream (37). We controlled this factor by including macrophytes in the causal networks of the recent period (Fig. 4*B*); that is, the effects of the remaining variables were inferred after considering the confounding effect of macrophyte abundance. After controlling for the effect of macrophytes, the sensitivity of all other taxa to climate variability still increased markedly (Figs. 3*B* and 4 *B*, ⑨–⑪). In fact, we found that macrophyte abundance was influenced by hydroclimatic conditions—it was strongly, negatively correlated to the magnitude of winter floods (Fig. 4 *B*, ④). Smaller and earlier winter floods in dry years (Fig. 1*B* and *SI Appendix*, Fig. S4) greatly facilitated seed germination and the expansion of macrophytes, consistent with previous findings in this system (36). The expansion of macrophytes and wetland plants under warmer and drier climate has also been reported in other streams around the world, particularly Mediterranean intermittent streams with dry summers like Sycamore Creek (52, 53). Furthermore, the observed structural changes in macroinvertebrate communities such as the increase of predatory Diptera (e.g., Ceratopogonidae) and the decrease of Oligochaeta and Chironomidae (*SI Appendix*, Table S4) in our study are remarkably consistent with whole-stream warming experiments (54), further confirming that the changes in community structure and dynamics reported here primarily resulted from climate change.

With future climate projected to feature more frequent extreme events and nonanalogous regimes, findings from our study are particularly relevant and alarming. Taking advantage of the long-term ecological monitoring of a climate-sensitive ecosystem, we analyzed the mechanisms underlying community stability historically and the breakdown of these mechanisms under a

changing climate. Multidimensional climatic stressors generated synergistic effects, and the resultant unprecedent habitat conditions invoked synchronous negative responses by taxa. This led to highly variable community dynamics from year to year and reduced taxa richness. While reorganizing species interactions might provide some buffer under species compositional change, we found that under a rapidly changing climate, when most species are already highly stressed, reorganized species interactions destabilized the community.

In our study system, these multiple destabilizing mechanisms have maintained the community in a new, highly variable regime for a decade. However, it might be still too early to determine whether this new state constitutes a new stable state or a long transient state toward another state. As climate continues to change, the ecosystem might experience further loss of native species but will also receive new species that are better adapted to the drier and warmer climate projected for this region (55). Some of the newly arriving species might alter interactions and feedbacks, which can dramatically modify the ecosystem (56). In Sycamore Creek, recently colonizing macrophytes have increased sediment trapping and bank stabilization, resulting in conversion of some reaches (not our study reach) to riverine wetlands, and transforming braided channels in some other parts of the system into single-threaded ones (37). Such large-scale biogeomorphic changes might require decades to achieve, leading to significant modification of the physical habitat for the macroinvertebrate community (57). Over the course of continuing climate change at century timescales and with geomorphic–hydrologic–ecologic feedbacks occurring at multiple spatial and temporal scales, many ecosystems might undergo series of successive transient states before reaching a new, resilient, self-sustaining state. In the case of this stream, that state may be an ephemeral wash or arroyo with little or no aquatic life. Patterns emerging from our study system, such as synchronous, nonlinear species responses to environment fluctuations, and enhanced fluctuations of aggregate community properties, may serve as diagnostics of ecosystem transformation (6). Mechanistic insights from this study can help better anticipate and cope with ecosystem state changes in response to ongoing climate change worldwide.

Materials and methods

Study Site and Observational Data. Our study site (33.75N, 111.50W; 610 m elevation) Sycamore Creek is located in the upper Sonoran Desert of central Arizona, USA, 32 km northeast of Phoenix (34). Sycamore Creek is a spatially intermittent desert stream draining a 505 km^2 watershed of mountainous terrain with elevations ranging from 427 to 2,164 m (*SI Appendix*, Fig. S1). The watershed receives ~267 mm of precipitation annually (averaging over 1980 to 2022; *SI Appendix*, Fig. S2*A*), most of which falls as rain during winter flood season (October-March) and the summer monsoon (late July-September) (33). Pan evaporation is very high, reaching 3,130 mm/year (4). Such precipitation and evaporation patterns lead to two distinct flood seasons: winter and late summer, with discharge peaks in winter often many times higher than those in the summer monsoon (*SI Appendix*, Fig. S2). The magnitude of floods varies widely from >100 $m^3\ s^{-1}$ (mean daily discharge) in wet years to 1 $m^3\ s^{-1}$ in dry years. A peak discharge of 1 $m^3\ s^{-1}$ is sufficient to "reset" the system by scouring and mobilization of bed materials (4). The hydrograph is very flashy, characterized by sudden, dramatic increases in discharge and rapid recession (58). Summer base flow (April-June), primarily fed by groundwater, is low (<0.05 $m^3\ s^{-1}$), due to high evapotranspiration and little precipitation; hence, most reaches are shallow (0 to 50 cm) and narrow (1 to 5 m) (58, 59). Such a highly variable flow regime at both interannual and intra-annual time scales is typical of most arid streams. Water temperature in March-July varies between 10 and 40 °C in 2018 to 2020 (*SI Appendix*, Fig. S14), depending on air temperature, discharge, and hydrodynamics (stagnant or running). In addition to temporal variability, the stream is spatially intermittent, as some parts of the stream dry out for several months in a year, while others are nearly perennial, with flowing water year-round in most years (40).

We compiled macroinvertebrate data collected in March-July during two periods: 1985 to 1999 and 2010 to 2019, a total of 118 field sampling events. Data were collected from the same gravel reach of ~200 m in length (*SI Appendix*, Fig. S1). The same standard procedure was applied for sampling and processing macroinvertebrates during the two periods except that a 7-cm diameter corer was used to collect samples between 2010-01-01 and 2014-03-11, while a 10-cm diameter corer was used for the remaining periods. Detailed description of field protocols can be found in the open database (32) and from previous studies (33, 40, 60). For historical data, specimens were counted and mostly identified to the family level with body size measured in 1997, while data from the recent period were refined to the genus level with measurements of body size. Worth noting is that it is almost infeasible to identify macroinvertebrates into species level given their superdiversity (51). Identification to family or genus level is a routine approach (25, 34, 54). To homogenize data of the two periods, we 1) multiplied the abundance between 2010-01-01 and 2014-03-11 by 1/0.49 to standardize corer area across the entire time series and 2) rescaled abundance data of the recent period to coarse levels that were consistent with identification resolution of the historical period (the first two columns in *SI Appendix*, Table S1). Furthermore, taking advantage of fine-resolution recent data, we calculated biomass of each taxon according to measured body size and length-biomass relationships reported in the literature (61, 62). Overall, we have 10 y of macroinvertebrate data in the historical period and 8 y of macroinvertebrate data in the recent period (stars in Fig. 1*A*). Each year, the frequency of sampling varies from weekly to monthly with up to five replicates for each sampling event.

To establish the relationship between climate change and response of the macroinvertebrate communities, we downloaded daily precipitation data (1980 to 2021) at Fountain Hills (~20 km from our study site) and used mean daily discharge data (1961 to 2021) from the USGS gauging station (ID: 09510200) ~12 km downstream of our study site to describe hydrological conditions. We classified each water year (from October to next September) into dry, normal, and wet years with 33 percentile and 67 percentile of annual mean discharge during 1980 to 2021. Due to a lack of long-term temperature data directly from Sycamore Creek, we used hourly air temperature data measured at the Phoenix airport (~50 km from Sycamore Creek, https://www.ncdc.noaa.gov/cdo-web/datasets/LCD/stations/WBAN:23183/detail) to represent air temperature trend at the study site since 1980. To better understand species interactions, we compiled algal and macrophyte data collected at the same time and the same reach with macroinvertebrate samplings, including diatoms, filamentous algae, blue-green algae, and macrophytes (https://ltreb-syc.gitlab.io/). We represented algal density by weighted average chlorophyll *a* concentration of diatoms, blue-green algae, and filamentous algae collectively. No algal data were available in 1989 and 2012 to match macroinvertebrate measurements of the 2 y. Last, we represented abundance of macrophytes using average width of macrophyte cover along transects (58). Macrophytes were mostly classified into genus or species level (*SI Appendix*, Table S2).

Time Series Analysis. We used a locally weighted linear regression model to quantify the trend of air temperature. We first calculated mean annual air temperature in 1980 to 2021 using hourly air temperature data. To estimate the temperature trend of a focal year, we identified temperature values of its 30 nearest neighboring years (i.e., 75% of the 40 y), and calculated the distance weight of each neighboring year using a tricubic function:

$$w(x) = \left(1 - \left|\frac{d(x, x')}{\max_i d(x_i, x')}\right|^3\right)^3, \quad [1]$$

where x' is a focal year, x is one of its neighboring years, $w(x)$ is the distance weight of a neighboring year x, $d(x, x')$ is Euclidean distance between x and x', and $\max_i d(x_i, x')$ is maximum distance between x' and its 30 neighboring years. With observed temperature and weights of 30 neighboring years, we estimated parameters of a locally weighted linear regression model and then calculated trended temperature in a focal year (Fig. 1*A*).

To characterize precipitation and flood events, we calculated annual mean precipitation and mean and peak discharge in the winter flood season (October-March). To represent intensity of drought of a year, we used number of zero-flow

days of a water year and number of zero-flow days between March and July (i.e., the sampling season, a dry period between winter flood and summer monsoon seasons) (Fig. 1*B*). To test whether these metrics significantly changed from the historical to the recent period (Fig. 1 *D* and *E*), we applied a modified Welch's *t* test with equivalent sample sizes to compensate for potential autocorrelation in time series (63). We also did a systematic evaluation of hydroclimatic regime alterations in the historical and recent periods with a wide range of metrics (information about the *t* test and its result is provided in *SI Appendix, Text S2*). To detect whether flow regimes in the two periods have distinct periodicities, we used wavelet analysis to obtain dominant periods of daily discharge time series (59, 64). The R package WaveletComp was used to compute wavelet power of periods ranging from 1 mo to 20 y on each day in 1980 to 2021 (Fig. 1*C*).

To visualize the interannual trajectory of the macroinvertebrate community, we used nonmetric multidimensional scaling (NMDS) to reduce high-dimensional community composition data (21 taxa groups/dimensions) to two-dimensional data (Fig. 3*C*). First, to homogenize data of the historical and recent periods, we classified macroinvertebrates into 21 taxa (genus, family, order, or subclass) using the coarse classification of the historical period (the second column in *SI Appendix*, Table S1). Second, to obtain yearly community composition, we calculated mean abundance of each group using all the samplings carried out over the sampling season (March–July) of a given year. Third, we performed a logarithmic transformation of abundance for each group to ensure that abundance change of the rare but ecologically important groups such as top predators was reflected in NMDS. We then ran NMDS using the R package vegan, where difference in the community composition between any 2 y was quantified by Bray–Curtis dissimilarity. Last, we checked the stress of NMDS and ensured it was under 0.1 (0.096) so that it was reasonable to interpret the community trajectory using two-dimensional data (34). We then calculated relative abundance of eight classes/orders (Fig. 3*C*) to better understand year-to-year community structural dynamics. To test whether macroinvertebrate richness altered between the two periods, we applied the modified Welch's *t* test (*SI Appendix, Text S2.2*) to yearly taxa richness data (Fig. 3*B*). We also applied the same NMDS method to analyze the interannual trajectory of algal and macrophyte communities (*SI Appendix*, Fig. S15).

We used VR to determine the presence and absence of compensatory dynamics in the interannual variability of the macroinvertebrate communities (11). We first obtained the annual mean biomass density of each taxon. We then calculate VR values of the historical period and recent period separately using the equation given by:

$$VR = \frac{var\left(\sum_{i=1}^{n} P_i\right)}{\sum_{i=1}^{n} var\left(P_i\right)}, \quad [2]$$

where n is the number of taxa, P_i is the annual mean biomass density of the ith taxa, and *var* is variance. A VR less than 1 indicates that the sum of covariances among species is negative, the evidence for compensatory dynamics. In contrast, a VR greater than 1 indicates synchronous dynamics. Additionally, we estimated a CI for each VR by resampling the community composition data using the block bootstrapping method (65). To quantify temporal stability of total biomass density of macroinvertebrate communities, we calculated the CV for each period and estimated its CI using the same bootstrapping approach.

Statistical Models. We used the Bayesian structural causal model framework to quantify direct and total effects of air temperature and hydrological conditions on macroinvertebrates and other ecological components (66, 67). Under this framework, we created causal networks (i.e., a directed acyclic graph, DAG) linking air temperature, magnitude of winter flood, intensity of summer drought, abundance of macrophytes, algal density, and macroinvertebrate abundance (Fig. 4). The DAGs represent our hypothesized causal relationships among these components informed by previous studies of this ecosystem (4, 33, 34, 37, 40, 58). We hypothesized no direct causal effect by macroinvertebrates on algae and macrophytes because of negligible grazing effects by macroinvertebrates in our study system according to previous studies (4, 33) (see *SI Appendix, Text S4.1* for justification of DAGs). Compared to the causal networks in the historical period (Fig. 4*A*), we added a new component, macrophytes into the causal networks in the recent period (Fig. 4*B*) to control for the confounding effects of macrophyte expansion after cattle removal in 2000 on macroinvertebrates. Macrophyte abundance affects algal abundance by shading and nutrient competition and is influenced by air temperature and magnitude of winter flood (36). We used the R package dagitty to test DAG-data consistency and identified the predictor variables to be included in statistical models when we estimated each direct or total effect within the causal networks (detailed information provided in *SI Appendix, Text S4*) (66, 68).

We first quantified the total and antecedent effects of summer drought on the abundance of eight taxonomic groups of macroinvertebrates (Fig. 2 *A* and *B*) using Bayesian multiple regression models with antecedent effects (38). In the historical period, macroinvertebrates were affected by both air temperature and summer drought (Fig. 4*A*), so the model conditioned on the variables air temperature to estimate the total effect of summer drought. While in the recent period, macroinvertebrates were additionally influenced by macrophytes (Fig. 4*B*), air temperature and macrophytes were both included in the model to control for their effects. To quantify the lag and strength of antecedent effects by summer drought (i.e., accumulative effect of multiyear drought), we included 2-y antecedent hydrological conditions into the multiple regression model. To investigate the effects of interannual climatic variability on macroinvertebrates, we incorporated a variable, timing of each sampling event into the model, to control for the effect of seasonal trend among multiple sampling events in each year. The likelihood function and the mean model are described as follows:

$$y_i \sim Normal\left(\mu_i, \sigma\right), \quad [3]$$

$$\mu_i = \alpha + \delta S_i + \beta T_{yr(i)} + \varphi P_i + \gamma\left(w_0 H_{0,yr(i)} + w_{-1} H_{-1,yr(i)} + w_{-2} H_{-2,yr(i)}\right), \quad [4]$$

where i indexes the sampling events ($i = 1, 2, 3, \ldots, 90$ over 10 y in the historical period; and $i = 1, 2, 3, \ldots, 28$ over 8 y in the recent period). i is nested within different years, indexed by yr ($yr = 1, 2, 3, \ldots, 10$ for the historical period; and $yr = 1, 2, 3, \ldots, 8$ for the recent period). y_i is the abundance of each macroinvertebrate taxonomic group in the sampling event i, and μ_i and σ are mean and SD of the likelihood function (Eq. **3**). α is intercept, S_i is timing of the sampling event i, represented by the number of days between the date of last winter flood [i.e., the start of spring succession in this stream (33)] and the date of the sampling event i, T_{yr} is mean air temperature during the sampling season in the year yr, and P_i is average width of macrophyte cover along transects in the sampling event i. The variable macrophyte P_i was omitted in the model for the historical period. δ, β, and φ are the effect size of the corresponding variables. γ is the total effect size of summer drought intensity. $H_{0,yr}$, $H_{-1,yr}$, and $H_{-2,yr}$ are intensity of summer drought of the current year (year yr), 1-y antecedent (yr-1), and 2-y antecedent (yr-2), respectively. w_0, w_{-1}, and w_{-2} are the corresponding weight parameters to be estimated by the model. They represent the relative importance of the corresponding year's hydrological condition. Here, we only considered antecedent hydrology of the previous 2 y because macroinvertebrates' lifespan is <2 y in this stream (40, 60). These weights were constrained to vary between 0 and 1, and $w_0 + w_{-1} + w_{-2} = 1$. To satisfy these constrains, we used Dirichlet distributions as the prior distributions for w_0, w_{-1}, and w_{-2}. We completed the model specification by assigning prior to all unknown, stochastic parameters. Each regression parameter $\alpha, \delta, \beta, \varphi$, and r was assigned a relatively noninformative prior: *Normal*(0, 5). We specified an exponential distribution for the SD describing the distribution of y_i such that $\sigma \sim exp(1)$. Finally, we chose a relatively noninformative Dirichlet prior for the vector of antecedent weights, $\boldsymbol{w} = \left(w_0, w_{-1}, w_{-2}\right)$, such that $\boldsymbol{w} \sim Dirichlet(\mathbf{1})$, where $\mathbf{1}$ is a vector of 1's of length 3.

Next, to estimate the total effects of air temperature on the abundance of each macroinvertebrate taxonomic group, we constructed linear regression models for the abundance conditioning on air temperature according to the hypothesized relationships in the causal networks (Fig. 4). Further, we used Bayesian multiple linear regressions to quantify the direct effect of each predictor variable on its response variable (i.e., each causal link) in the causal networks (Fig. 4). Whenever the intensity of summer drought was conditioned on in the regression models, we also included its antecedent effects, that is 2-y antecedent summer drought conditions using the same method shown in Eq. **4**.

To directly compare effect sizes between the historical and the recent periods, we standardized all predictor and response variables using their mean and SD in the historical period and built separate regression models for the two periods. All the regression models used the similar likelihood functions as shown in Eq. **3**. We coded the models in the R package Rstan. For each model variant, we sampled the posterior parameter space using the Hamiltonian Monte Carlo. We assessed model convergence using the Gelman and Rubin diagnostic (69). We obtained >2,000 effective samples to construct posterior distributions of parameters. We reported the posterior mean and 90% credible intervals, defined by the 5th and 95th percentiles as well as the amount of variation in response variables explained by predictors (i.e., R^2).

Data, Materials, and Software Availability. All the data used in this study are published online (https://ltreb-syc.gitlab.io/) (70–73) except for the algal community data in the historical period which are available from a repository (osf.io/hd3rj/) (74).

ACKNOWLEDGMENTS. We thank Vadim Karatayev and the two anonymous reviewers for their insightful and constructive comments on the manuscript. We thank Daniel Allen, Stevan Earl, Brian Gill, Anya Metcalfe, Scott Starr, and Sophia Bonjour for their help with quality assurance/quality control of the macroinvertebrate data. We thank Zhanzhong Wang for assisting in plotting all the figures in this paper. We acknowledge many students, technicians, and postdocs contributing to data collection over decades. This research was supported by the Virginia M Ullman Chair in Ecology at Arizona State University, NSF grants #1442522, 1457227, and 2040194 to N.B.G., and NSF grant #1924378 to X.D.

Author affiliations: [a]Department of Environmental Science and Policy, University of California, Davis, CA 95616; [b]School of Life Sciences, Arizona State University, Tempe, AZ 85287; and [c]Department of Entomology & Nematology, University of California, Davis, CA 95616

1. P. Chesson, Mechanisms of maintenance of species diversity. *Annu. Rev. Ecol. Syst.* **31**, 343–366 (2000).
2. K. S. McCann, The diversity–stability debate. *Nature* **405**, 228–233 (2000).
3. Y. Bai, X. Han, J. Wu, Z. Chen, L. Li, Ecosystem stability and compensatory effects in the Inner Mongolia grassland. *Nature* **431**, 181–184 (2004).
4. S. G. Fisher, L. J. Gray, N. B. Grimm, D. E. Busch, Temporal succession in a desert stream ecosystem following flash flooding. *Ecol. Monogr.* **52**, 93–110 (1982).
5. C. S. Holling, Resilience and stability of ecological systems. *Annu. Rev. Ecol. Syst.* **4**, 1–23 (1973).
6. S. M. Sundstrom *et al.*, The distribution and role of functional abundance in cross-scale resilience. *Ecology* **99**, 2421–2432 (2018).
7. G. Peterson, C. R. Allen, C. S. Holling, Ecological resilience, biodiversity, and scale. *Ecosystems* **1**, 6–18 (1998).
8. M. Loreau *et al.*, Biodiversity and ecosystem functioning: Current knowledge and future challenges. *Science* **294**, 804–808 (2001).
9. A. R. Ives, K. Gross, J. L. Klug, Stability and variability in competitive communities. *Science* **286**, 542–544 (1999).
10. S. Yachi, M. Loreau, Biodiversity and ecosystem productivity in a fluctuating environment: The insurance hypothesis. *Proc. Natl. Acad. Sci. U.S.A.* **96**, 1463–1468 (1999).
11. A. Gonzalez, M. Loreau, The causes and consequences of compensatory dynamics in ecological communities. *Annu. Rev. Ecol. Evol. Syst.* **40**, 393–414 (2009).
12. R. T. Paine, A note on trophic complexity and community stability. *Am. Nat.* **103**, 91–93 (1969).
13. K. McCann, A. Hastings, G. R. Huxel, Weak trophic interactions and the balance of nature. *Nature* **395**, 794–798 (1998).
14. J. P. DeLong, T. C. Hanley, J. P. Gibert, L. M. Puth, D. M. Post, Life history traits and functional processes generate multiple pathways to ecological stability. *Ecology* **99**, 5–12 (2018).
15. B. G. Miner, S. E. Sultan, S. G. Morgan, D. K. Padilla, R. A. Relyea, Ecological consequences of phenotypic plasticity. *Trends Ecol. Evol.* **20**, 685–692 (2005).
16. W. R. L. Anderegg *et al.*, Pervasive drought legacies in forest ecosystems and their implications for carbon cycle models. *Science* **349**, 528–532 (2015).
17. E. Post, *Ecology of Climate Change* (Princeton University Press, 2013).
18. C. Bellard, C. Bertelsmeier, P. Leadley, W. Thuiller, F. Courchamp, Impacts of climate change on the future of biodiversity. *Ecol. Lett.* **15**, 365–377 (2012).
19. J. M. Alexander, J. M. Diez, J. M. Levine, Novel competitors shape species' responses to climate change. *Nature* **525**, 515–518 (2015).
20. T. J. Bartley *et al.*, Food web rewiring in a changing world. *Nat. Ecol. Evol.* **3**, 345–354 (2019).
21. J. H. Brown, T. G. Whitham, S. K. Morgan Ernest, C. A. Gehring, Complex species interactions and the dynamics of ecological systems: Long-term experiments. *Science* **293**, 643–650 (2001).
22. J. M. Tylianakis, R. K. Didham, J. Bascompte, D. A. Wardle, Global change and species interactions in terrestrial ecosystems. *Ecol. Lett.* **11**, 1351–1363 (2008).
23. J. A. Estes *et al.*, Trophic downgrading of planet earth. *Science* **333**, 301–306 (2011).
24. K. B. Suttle, M. A. Thomsen, M. E. Power, Species interactions reverse grassland responses to changing climate. *Science* **315**, 640–642 (2007).
25. X. Lu *et al.*, Drought rewires the cores of food webs. *Nat. Clim. Change* **6**, 875–878 (2016).
26. R. A. Garcia, M. Cabeza, C. Rahbek, M. B. Araújo, Multiple dimensions of climate change and their implications for biodiversity. *Science* **344**, 1247579 (2014).
27. D. Chen *et al.*, "Framing, context, and methods" in *IPCC, 2021: Climate Change 2021: The Physical Science Basis. Contribution of Working Group I to the Sixth Assessment Report of the Intergovernmental Panel on Climate Change*, V. Masson-Delmotte *et al.*, Eds. (Cambridge University Press, Cambridge, United Kingdom and New York, NY, USA, 2021).
28. C. R. Ebel *et al.*, Herbivory and drought reduce the temporal stability of herbaceous cover by increasing synchrony in a semi-arid savanna. *Front. Ecol. Evol.* **10**, 1–17 (2022).
29. A. R. Ives, S. R. Carpenter, Stability and diversity of ecosystems. *Science* **317**, 58–62 (2007).
30. M. Winder, D. E. Schindler, Climate change uncouples trophic interactions in an aquatic ecosystem. *Ecology* **85**, 2100–2106 (2004).
31. G. E. Maurer, A. J. Hallmark, R. F. Brown, O. E. Sala, S. L. Collins, Sensitivity of primary production to precipitation across the United States. *Ecol. Lett.* **23**, 527–536 (2020).
32. N. Grimm *et al.*, Long-term monitoring of macroinvertebrates in Sycamore Creek, Arizona, USA (2010–2019) (Version 2, 2021), Environment Data Initiation.
33. N. B. Grimm, S. G. Fisher, Stability of periphyton and macroinvertebrates to disturbance by flash floods in a desert stream. *J. North Am. Benthol. Soc.* **8**, 293–307 (1989).
34. R. A. Sponseller, N. B. Grimm, A. J. Boulton, J. L. Sabo, Responses of macroinvertebrate communities to long-term flow variability in a Sonoran Desert stream. *Glob. Change Biol.* **16**, 2891–2900 (2010).
35. D. R. Cayan *et al.*, Future dryness in the Southwest US and the hydrology of the early 21st century drought. *Proc. Natl. Acad. Sci. U.S.A.* **107**, 21271–21276 (2010).
36. X. Dong, N. B. Grimm, J. B. Heffernan, R. Muneepeerakul, Interactions between physical template and self-organization shape plant dynamics in a stream ecosystem. *Ecosystems* **23**, 891–905 (2020).
37. J. B. Heffernan, Wetlands as an alternative stable state in desert streams. *Ecology* **89**, 1261–1271 (2008).
38. K. Ogle *et al.*, Quantifying ecological memory in plant and ecosystem processes. *Ecol. Lett.* **18**, 221–235 (2015).
39. J. H. Thorp, A. P. Covich, *Ecology and Classification of North American Freshwater Invertebrates* (Academic press, 2009).
40. E. H. Stanley, D. L. Buschman, A. J. Boulton, N. B. Grimm, S. G. Fisher, Invertebrate resistance and resilience to intermittency in a desert stream. *Am. Midl. Nat.* **131**, 288–300 (1994).
41. Y. Vadeboncoeur, M. E. Power, Attached algae: The cryptic base of inverted trophic pyramids in freshwaters. *Annu. Rev. Ecol. Evol. Syst.* **48**, 255–279 (2017).
42. E. Grman, J. A. Lau, D. R. Schoolmaster, K. L. Gross, Mechanisms contributing to stability in ecosystem function depend on the environmental context. *Ecol. Lett.* **13**, 1400–1410 (2010).
43. M. T. Bogan, K. S. Boersma, D. A. Lytle, Resistance and resilience of invertebrate communities to seasonal and supraseasonal drought in arid-land headwater streams. *Freshw. Biol.* **60**, 2547–2558 (2015).
44. J. Constantz, Interaction between stream temperature, streamflow, and groundwater exchanges in alpine streams. *Water Resour. Res.* **34**, 1609–1615 (1998).
45. W. K. Dodds, B. J. F. Biggs, Water velocity attenuation by stream periphyton and macrophytes in relation to growth form and architecture. *J. North Am. Benthol. Soc.* **21**, 2–15 (2002).
46. S. Folegot *et al.*, Low flow controls on stream thermal dynamics. *Limnologica* **68**, 157–167 (2018).
47. S. L. Castle *et al.*, Groundwater depletion during drought threatens future water security of the Colorado River Basin. *Geophys. Res. Lett.* **41**, 5904–5911 (2014).
48. A. Gonzalez, O. De Feo, "Environmental variability modulates the insurance effects of diversity in non-equilibrium communities" in *The Impact of Environmental Variability on Ecological Systems* (Springer, 2007), pp. 159–177.
49. M. E. Ledger, L. E. Brown, F. K. Edwards, A. M. Milner, G. Woodward, Drought alters the structure and functioning of complex food webs. *Nat. Clim. Change* **3**, 223–227 (2013).
50. M. E. Power, M. S. Parker, W. E. Dietrich, Seasonal reassembly of a river food web: Floods, droughts, and impacts of fish. *Ecol. Monogr.* **78**, 263–282 (2008).
51. R. W. Merritt, K. W. Cummins, *An Introduction to the Aquatic Insects of North America* (Kendall Hunt, 1996).
52. C. G. Westwood, R. M. Teeuw, P. M. Wade, N. T. H. Holmes, P. Guyard, Influences of environmental conditions on macrophyte communities in drought-affected headwater streams. *River Res. Appl.* **22**, 703–726 (2006).
53. P. Manolaki, K. Guo, C. Vieira, E. Papastergiadou, T. Riis, Hydromorphology as a controlling factor of macrophytes assemblage structure and functional traits in the semi-arid European Mediterranean streams. *Sci. Total Environ.* **703**, 134658 (2020).
54. D. Nelson *et al.*, Experimental whole-stream warming alters community size structure. *Glob. Chang. Biol.* **23**, 2618–2628 (2017).
55. B. I. Cook, T. R. Ault, J. E. Smerdon, Unprecedented 21st century drought risk in the American Southwest and Central Plains. *Sci. Adv.* **1**, e1400082 (2015).
56. S. T. Jackson, Transformational ecology and climate change. *Science* **373**, 1085–1086 (2021).
57. D. Corenblit *et al.*, Feedbacks between geomorphology and biota controlling Earth surface processes and landforms: A review of foundation concepts and current understandings. *Earth-Science Rev.* **106**, 307–331 (2011).
58. X. Dong, N. B. Grimm, K. Ogle, J. Franklin, Temporal variability in hydrology modifies the influence of geomorphology on wetland distribution along a desert stream. *J. Ecol.* **104**, 18–30 (2016).
59. X. Dong, A. Ruhí, N. B. Grimm, Evidence for self-organization in determining spatial patterns of stream nutrients, despite primacy of the geomorphic template. *Proc. Natl. Acad. Sci. U.S.A.* **114**, E4744–E4752 (2017).
60. A. J. Boulton, C. G. Peterson, N. B. Grimm, S. G. Fisher, Stability of an aquatic macroinvertebrate community in a multiyear hydrologic disturbance regime. *Ecology* **73**, 2192–2207 (1992).
61. A. C. Benke, A. D. Huryn, L. A. Smock, J. B. Wallace, Length-mass relationships for freshwater macroinvertebrates in North America with particular reference to the southeastern United States. *J. North Am. Benthol. Soc.* **18**, 308–343 (1999).
62. G. Méthot *et al.*, Macroinvertebrate size–mass relationships: How specific should they be? *Freshw. Sci.* **31**, 750–764 (2012).
63. P. O'Shaughnessy, J. E. Cavanaugh, Performing t-tests to compare autocorrelated time series data collected from direct-reading instruments. *J. Occup. Environ. Hyg.* **12**, 743–752 (2015).
64. C. Torrence, G. P. Compo, A practical guide to wavelet analysis. *Bull. Am. Meteorol. Soc.* **79**, 61–78 (1998).
65. A. C. Davison, D. V. Hinkley, *Bootstrap Methods and Their Application* (Cambridge University Press, 1997).
66. J. Pearl, Causal inference in statistics: An overview. *Stat. Surv.* **3**, 96–146 (2009).
67. S. Arif, M. A. MacNeil, Applying the structural causal model framework for observational causal inference in ecology. *Ecol. Monogr.* **93**, e1554 (2022).
68. R. McElreath, *Statistical Rethinking: A Bayesian Course with Examples in R and Stan* (Chapman and Hall/CRC, 2018).

69. A. Gelman, D. B. Rubin, Inference from iterative simulation using multiple sequences. *Stat. Sci.* **7**, 457–472 (1992).
70. N. Grimm *et al.*, Long-term monitoring of macroinvertebrates in Sycamore Creek, Arizona, USA (2010–2019) ver 2. Environmental Data Initiative. https://doi.org/10.6073/pasta/93e6b8ce17d327c696b7716c850910b2. Accessed 25 May 2021.
71. N. Grimm, S. Fisher, Macroinvertebrate collections following floods in Sycamore Creek, Arizona, USA 1985-1999 ver 8. Environmental Data Initiative. https://doi.org/10.6073/pasta/8689be281880702d93dff1e3f5c213c1. Accessed 25 May 2021.
72. N. Grimm *et al.*, Long-term record of wetted area, substrate type, and plant features in Sycamore Creek, Arizona, USA (2010-2020) ver 1. Environmental Data Initiative. https://doi.org/10.6073/pasta/20ac05ad5de6b1dd53a1ab28fc79b232. Accessed 25 May 2021.
73. N. Grimm *et al.*, Long-term measurements of algal biomass in Sycamore Creek, Arizona, USA (2011-2019) ver 1. Environmental Data Initiative. https://doi.org/10.6073/pasta/cf8a4b7fc8605fe6e42959e7ef1b7f4c. Accessed 25 May 2021.
74. J. Wang, Sycamore Creek. OSF. https://osf.io/hd3rj/. Deposited 17 February 2023.